A new method for true and spurious eigensolutions of arbitrary cavities using the combined Helmholtz exterior integral equation formulation method

I. L. Chen
Department of Naval Architecture, National Kaohsiung Institute of Marine Technology, Kaohsiung, Taiwan

J. T. Chen,[a] S. R. Kuo, and M. T. Liang
Department of Harbor and River Engineering, National Taiwan Ocean University, P.O. Box 7-59, Keelung, Taiwan

Integral equation methods have been widely used to solve interior eigenproblems and exterior acoustic problems (radiation and scattering). It was recently found that the real-part boundary element method (BEM) for the interior problem results in spurious eigensolutions if the singular (UT) or the hypersingular (LM) equation is used alone. The real-part BEM results in spurious solutions for interior problems in a similar way that the singular integral equation (UT method) results in fictitious solutions for the exterior problem. To solve this problem, a Combined Helmholtz Exterior integral Equation Formulation method (CHEEF) is proposed. Based on the CHEEF method, the spurious solutions can be filtered out if additional constraints from the exterior points are chosen carefully. Finally, two examples for the eigensolutions of circular and rectangular cavities are considered. The optimum numbers and proper positions for selecting the points in the exterior domain are analytically studied. Also, numerical experiments were designed to verify the analytical results. It is worth pointing out that the nodal line of radiation mode of a circle can be rotated due to symmetry, while the nodal line of the rectangular is on a fixed position. © *2001 Acoustical Society of America.* [DOI: 10.1121/1.1349187]

PACS numbers: 43.40.At [PJR]

I. INTRODUCTION

Acoustic problems are generally modeled using the wave equation, which is transient, or by the Helmholtz equation, which is time harmonic. While the solution to the original boundary value problem in the domain exterior to the boundary is perfectly unique for all wave numbers, this is not the case for the corresponding integral equation formulation, which breaks down at certain frequencies known as irregular frequencies or fictitious frequencies. This problem is completely nonphysical because there are no eigenvalues for the exterior problems. Schenck[1] proposed a Combined Helmholtz Interior integral Equation Formulation (CHIEF) method, which is easy to implement and is efficient but still has some drawbacks. A review article by Benthien and Schenck[2] is referenced. In the case of a fictitious frequency, the resulting coefficient matrix for the exterior acoustic problems becomes singular or ill-conditioned. This means that the boundary integral equations are not linearly independent and the matrix is rank deficient. In order to determine a unique solution, additional constraints for the system of equations are required. The missing constraints or equations can be found by applying the integral equation on a number of points located outside of the domain of interest. When these equations are added to the system of equations, we have an overdetermined system of equations which can be

solved in a least-squares sense. Schenck[1] introduced this method and proved that the resulting solution is unique. But, how can we decide where to place the interior points efficiently and how many numbers of extra equations are needed? When an interior point is placed on the node of the associated interior nodes in CHIEF, it will not add an effective constraint to the system of equations, i.e., the extra equation is not linearly independent. For a general geometry, these nodal lines are not known *a priori* and this has been one of the difficulties of this method. Particularly, the problem becomes worse for the high frequency range. Wu *et al.*[3] introduced a method called CHIEF-block, in which the interior integral equation is satisfied in a weighted residual sense over a small region, called blocks, instead of discrete points. Since the interior eigensolutions cannot have a nodal block, this technique is effective. Juhl[4] and Poulin[5] proposed the CHIEF method in conjunction with the singular value decomposition (SVD) technique. This method is easy and efficient and produces a unique solution for the exterior problem.

For interior problems, eigensolutions are often encountered not only in vibration problems but also in acoustics. Since exact solutions are not always available, numerical methods are needed. Based on the complex-valued boundary element method (BEM),[6] the eigenvalues and eigenmodes can be determined. Nevertheless, complex computation is time consuming and not simple. To avoid complex computation, Nowak and Neves[7] proposed a multiple reciprocity method (MRM) in real-domain computation only. Tai and

[a]Author to whom correspondence should be addressed; electronic mail: jtchen@mail.ntou.edu.tw

Shaw[8] employed only real-part kernels to solve the eigenproblem. A simplified method using only the real-part or imaginary-part kernel was also presented by De Mey.[9] Although De Mey found that the zeros for a real-part determinant may be different from those for an imaginary-part determinant, the spurious solutions are not discovered if only a real-part formulation is employed. For a membrane vibration problem, Hutchinson[10] also employed real-part kernels to solve the membrane vibration. He found the spurious modes and proposed a filtering-out technique by examining the modal shapes. However, this technique may fail in some cases discussed by Chen et al.[11–13] This method using only the real-part BEM was later found to be equivalent to the multiple reciprocity method (MRM) if the zeroth-order fundamental solution in the MRM is properly chosen.[13] Chen and Wong[14] found that the MRM also results in spurious eigensolutions for one-dimensional examples. Numerical experiments using only the real-part kernels[15] were performed for a two-dimensional case. The spurious solutions in MRM[16–18] and real-part BEM[19] were filtered out using the SVD technique. The relations among the conventional MRM, complete MRM, real-part BEM, and complex-valued BEM were discussed by Chen.[13] It is obvious that one advantage of using only the real-part kernels is that real-valued computation is considered instead of complex-valued computation as used in the complex-valued BEM. Another benefit is that the lengthy derivation for the MRM can be avoided. However, two drawbacks of the real formulation have been found to be the occurrence of spurious eigenvalues as mentioned in Refs. 14–16 and 19, and the failure when it is applied to problems with a degenerate boundary. To deal with those two problems, the framework of a real-part dual BEM was constructed to filter out the spurious eigenvalues and to avoid the nonunique solution for problems with a degenerate boundary at the same time. As for the latter problem, the dual formulation[20] is a key step method to solve the problems with a degenerate boundary. As for the former problem, the reason why spurious eigenvalues occur in the MRM or the real-part BEM is the loss of the constraints in the imaginary part, which was investigated by Yieh et al.[21] The smaller number of constraint equations makes the solution space larger. The spurious eigensolutions can be filtered out using many alternatives: e.g., the complex-valued formulation, the domain partition technique,[22] and the dual formulation in conjunction with SVD.[11,16–18] Using the dual MRM or the real-part dual BEM, spurious eigenvalues can be filtered out by checking the residue between the singular and hypersingular equations.[14,23] Both the dual MRM method[16] and the real-part dual BEM[19] in conjunction with the SVD technique must calculate a $4N$ by $2N$ matrix, where $2N$ is the number of elements. In the series of work by Chen's group,[16,19,24] the multiplicity for true eigenvalues was also determined. By employing the present CHEEF method, the missing constraints can be found again by applying the integral equations on a number of points located in the exterior domain. It is necessary to determine a matrix with only dimension $(2N+1)$ by $2N$ or $(2N+2)$ by $2N$ for CHEEF instead of $4N \times 2N$ in dual formulation.
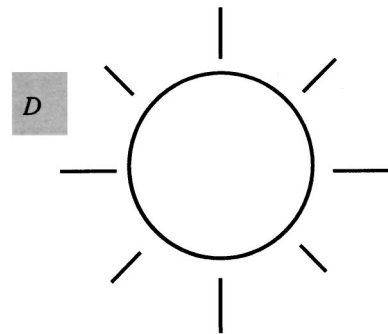

FIG. 1. The definitions of the exterior domain.

In this study, we employed the CHEEF BEM to filter out the spurious solutions for two-dimensional interior acoustic problems. The corresponding relationship between the CHIEF and CHEEF methods will be discussed. The optimum number and position for the interior points will be studied analytically and verified numerically. After assembling the CHEEF equations, an SVD technique is employed to determine the eigenvalues, multiplicity, and boundary modes. The boundary modes can be extracted easily from the right unitary matrix in SVD. Two examples for circular and rectangular domains with the Dirichlet boundary conditions are demonstrated to check the validity of the proposed method analytically and numerically.

II. REVIEW OF THE CHIEF METHOD FOR A TWO-DIMENSIONAL EXTERIOR ACOUSTIC PROBLEM USING THE SINGULAR INTEGRAL FORMULATION

Consider an acoustic problem which has the following governing equation:

$$\nabla^2 u(\mathbf{x}) + k^2 u(\mathbf{x}) = 0, \quad \mathbf{x} \in D, \tag{1}$$

where D is the domain of interest, as shown in Fig. 1, $\mathbf{x}$ is the domain point, u is the acoustic pressure, and k is the wave number defined by the angular frequency divided by the sound speed. The boundary conditions are shown as follows:

$$u(\mathbf{x}) = \bar{u}, \quad \mathbf{x} \in B, \tag{2}$$

where B denotes the boundary enclosing D.

The acoustic field can be described using the following integral equation:[25]

$$2\pi u(\mathbf{x}) = \int_B T(\mathbf{s},\mathbf{x}) u(\mathbf{s}) dB(\mathbf{s})$$
$$- \int_B U(\mathbf{s},\mathbf{x}) \frac{\partial u(\mathbf{s})}{\partial n_{\mathbf{s}}} dB(\mathbf{s}), \quad \mathbf{x} \in D, \tag{3}$$

where $T(\mathbf{s},\mathbf{x})$ is defined using

$$T(\mathbf{s},\mathbf{x}) \equiv \frac{\partial U(\mathbf{s},\mathbf{x})}{\partial n_{\mathbf{s}}}, \tag{4}$$

in which $n_{\mathbf{s}}$ represents the outnormal direction at point $\mathbf{s}$ on the boundary and $U(\mathbf{s},\mathbf{x})$ is the fundamental solution which satisfies

$$\nabla^2 U(\mathbf{x},\mathbf{s}) + k^2 U(\mathbf{x},\mathbf{s}) = \delta(\mathbf{x}-\mathbf{s}), \quad \mathbf{x} \in D, \tag{5}$$

where $\delta(\mathbf{x}-\mathbf{s})$ is the Dirac delta function. By moving the field point x in Eq. (3) to the smooth boundary, the boundary integral equation for the boundary point can be obtained as follows:

$$\pi u(\mathbf{x}) = \text{C.P.V.} \int_B T(\mathbf{s},\mathbf{x}) u(\mathbf{s}) dB(\mathbf{s})$$

$$- \text{R.P.V.} \int_B U(\mathbf{s},\mathbf{x}) \frac{\partial u(\mathbf{s})}{\partial n_{\mathbf{s}}} dB(\mathbf{s}), \quad \mathbf{x} \in B, \quad (6)$$

where C.P.V. is the Cauchy principal value and R.P.V. is the Riemann principal value. By moving the point x from the exterior domain (D^e) to the interior domain (D^i), the boundary integral equation for the interior point can be obtained as follows:

$$0 = \int_B T(\mathbf{s},\mathbf{x}) u(\mathbf{s}) dB(\mathbf{s}) - \int_B U(\mathbf{s},\mathbf{x}) \frac{\partial u(\mathbf{s})}{\partial n_{\mathbf{s}}} dB(\mathbf{s}), \quad \mathbf{x} \in D^i. \quad (7)$$

After Eq. (7) is added to Eq. (6), we can produce an overdetermined system of equations.

By discretizing the boundary B into the boundary elements in Eq. (6), we have the algebraic system as follows:

$$\pi\{u\} = [T]\{u\} - [U]\{t\}, \quad (8)$$

where $t = \partial u(s)/\partial n_s$, and the $[U]$ and $[T]$ matrices are the corresponding influence coefficient matrices resulting from the U and T kernels, respectively. The detailed derivation can be found in Refs. 15 and 23. Equation (8) can be rewritten as

$$[\bar{T}]\{u\} = [U]\{t\}, \quad (9)$$

where $[\bar{T}] = [T] - \pi[I]$. For simplicity, the Dirichlet radiation problem, i.e., $\{u\} = \bar{u}$ is considered in Eq. (9). Therefore, we obtain the following equation:

$$[U]\{t\} = [\bar{T}]\{\bar{u}\}. \quad (10)$$

We can rewrite the singular equations as follows:

$$[U^B(k)]_{2N \times 2N}\{t\}_{2N \times 1} = \{q_1\}_{2N \times 1}, \quad (11)$$

where the superscript B denotes the boundary, and $\{q_1\} = [\bar{T}]\{\bar{u}\}$ and $2N$ is the number of boundary elements. Similarly, discretization of Eq. (7) can have

$$[U^I(k)]_{a \times 2N}\{t\}_{2N \times 1} = \{q_2\}_{a \times 1}, \quad (12)$$

where $\{q_2\} = [T]\{\bar{u}\}$, subscript a indicates the number of additional interior points and the number of selected points $a \geq 1$, and superscript I denotes the interior domain. We can merge the two matrices in Eqs. (11) and (12) together to obtain an overdetermined system

$$[C(k)]_{(2N+a) \times 2N}\{u\}_{2N \times 1} = \{q\}_{(2N+a) \times 1}, \quad (13)$$

where $\{q\}$ is assembled by $\{q_1\}$ and $\{q_2\}$, the $[C(k)]$ matrix is composed by the $[U^B]$ and $[U^I]$ matrices as shown below

$$[C(k)]_{(2N+a) \times 2N} = \begin{bmatrix} U^B(k) \\ U^I(k) \end{bmatrix} \quad (14)$$

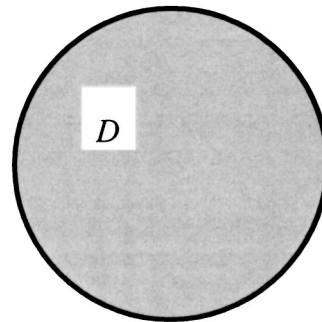for the Dirichlet problem. Therefore, an over-determined

FIG. 2. The definitions of interior domain.

system is obtained to ensure a unique solution. Similarly, we can extend the Dirichlet problem to the Neumann problem.

III. REVIEW OF THE REAL-PART DUAL BEM FOR A TWO-DIMENSIONAL INTERIOR ACOUSTIC PROBLEM

According to the findings by Yeih $et\ al.$[21] and Kamiya $et\ al.$,[26] the series forms of the kernels in the MRM are no more than the real parts of the closed-form kernels in the complex-valued BEM. The closed-form kernels for the real-part of BEM are shown below

$$U(\mathbf{s},\mathbf{x}) = \frac{\pi Y_0(kr)}{2}, \quad (15)$$

$$T(\mathbf{s},\mathbf{x}) = \frac{k\pi}{2} Y_1(kr) \frac{y_i n_i}{r}, \quad (16)$$

where $Y_n(kr)$ denotes the second-order kind Bessel function with order n, n_i denote the ith components of the normal vectors at $\mathbf{s}$, and $y_i = s_i - x_i$.

In order to filter out the spurious eigenvalues, Chen and Wong[14] developed the dual method by taking the normal derivative of the first equation [Eq. (3)]. The second equation of the dual boundary integral equation for the domain point x can be derived as follows:

$$2\pi \frac{\partial u(\mathbf{x})}{\partial n_{\mathbf{x}}} = \int_B M(\mathbf{s},\mathbf{x}) u(\mathbf{s}) dB(\mathbf{s})$$

$$- \int_B L(\mathbf{s},\mathbf{x}) \frac{\partial u(\mathbf{s})}{\partial n_{\mathbf{s}}} dB(\mathbf{s}), \quad \mathbf{x} \in D, \quad (17)$$

where D is the domain of interest as shown in Fig. 2, and

$$L(\mathbf{s},\mathbf{x}) \equiv \frac{\partial U(\mathbf{s},\mathbf{x})}{\partial n_{\mathbf{x}}}, \quad (18)$$

$$M(\mathbf{s},\mathbf{x}) \equiv \frac{\partial^2 U(\mathbf{s},\mathbf{x})}{\partial n_{\mathbf{x}} \partial n_{\mathbf{s}}}, \quad (19)$$

in which $n_{\mathbf{x}}$ represents the outnormal direction at point $\mathbf{x}$. For the real-part BEM, the closed forms for the L and M kernels are shown below

$$L(\mathbf{s},\mathbf{x}) = \frac{-k\pi}{2} Y_1(kr) \frac{y_i \bar{n}_i}{r}, \quad (20)$$

$$M(\mathbf{s},\mathbf{x}) = \frac{k\pi}{2}\left\{ -k\frac{Y_2(kr)}{r^2}y_iy_jn_i\bar{n}_j + \frac{Y_1(kr)}{r}n_i\bar{n}_i \right\}. \tag{21}$$

By moving the field point x in Eq. (17) to the smooth boundary, the boundary integral equations for the boundary point can be obtained as follows:

$$\pi\frac{\partial u(\mathbf{x})}{\partial n_{\mathbf{x}}} = \text{H.P.V.}\int_B M(\mathbf{s},\mathbf{x})u(s)dB(\mathbf{s})$$
$$-\text{C.P.V.}\int_B L(\mathbf{s},\mathbf{x})\frac{\partial u(\mathbf{s})}{\partial n_{\mathbf{s}}}dB(\mathbf{s}), \quad \mathbf{x}\in B, \tag{22}$$

where H.P.V. is the Hadamard (Mangler) principal value. By moving the interior point x to the exterior domain, the boundary integral equations for the exterior point can be obtained as follows:

$$0 = \int_B M(\mathbf{s},\mathbf{x})u(\mathbf{s})dB(\mathbf{s}) - \int_B L(\mathbf{s},\mathbf{x})\frac{\partial u(\mathbf{s})}{\partial n_{\mathbf{s}}}dB(\mathbf{s}), \quad \mathbf{x}\in D^e. \tag{23}$$

By discretizing the boundary B into boundary elements in Eq. (6) and Eq. (22), we have the dual algebraic system as follows:

$$\pi\{u\} = [T]\{u\} - [U]\{t\}, \tag{24}$$

$$\pi\{t\} = [M]\{u\} - [L]\{t\}, \tag{25}$$

where the $[U]$, $[T]$, $[L]$, and $[M]$ matrices are the corresponding influence coefficient matrices resulting from the U, T, L, and M kernels, respectively. Equation (24) and Eq. (25) can be rewritten as

$$[\bar{T}]\{u\} = [U]\{t\}, \tag{26}$$

$$[\bar{L}]\{t\} = [M]\{u\}, \tag{27}$$

where $[\bar{T}] = [T] - \pi[I]$ and $[\bar{L}] = [L] + \pi[I]$. For the Neumann problem, the eigenequation obtained from the UT and LM equations in Eqs. (26) and (27) can be rewritten as

$$[\bar{T}(k)]_{2N\times 2N}\{u\}_{2N\times 1} = \{0\}, \tag{28}$$

$$[M(k)]_{2N\times 2N}\{u\}_{2N\times 1} = \{0\}. \tag{29}$$

By employing the real-part dual BEM, we merge the two matrices in Eqs. (28) and (29) together to obtain an overdetermined system

$$[A(k)]_{4N\times 2N}\{u\}_{2N\times 1} = \{0\}, \tag{30}$$

where the $[A(k)]$ matrix is assembled by the $[\bar{T}]$ and $[M]$ matrices as shown below:

$$[A(k)]_{4N\times 2N} = \begin{bmatrix} \bar{T}(k) \\ M(k) \end{bmatrix} \tag{31}$$

for the Neumann problem. Also, an overdetermined system is obtained. Similarly, we can extend the Neumann problem to the Dirichlet problem. To distinguish spurious eigenvalues, we can use the SVD technique.[16–19] Using the real-part dual BEM, spurious eigenvalues can be filtered out. The main advantage of this method is that it can solve problems

in the real domain. However, the dimension of $[A]$ is $4N$ by $2N$. To reduce the dimension, the CHEEF method is proposed in the following section.

IV. THE CHEEF METHOD FOR AN INTERIOR TWO-DIMENSIONAL ACOUSTIC PROBLEM IN CONJUNCTION WITH SVD TECHNIQUE

Based on the concept of the CHIEF method, we extend the CHIEF for exterior problems to the CHEEF method for interior problems. Since only the real-part formulation (MRM or real-part BEM) is of concern, one approach to obtaining enough constraints for the eigenequation instead of obtaining the imaginary part of the complex-valued formulation is to derive additional equations on exterior points. This method is similar to the CHIEF method. For simplicity, we will deal with the Dirichlet problem. Therefore, we can obtain the following equation:

$$[U(k)]\{t\} = \{0\}. \tag{32}$$

Now, we present a more efficient way to filter out spurious eigenvalues which can avoid determining the spurious boundary mode in advance. We can rewrite the singular equation and additional equations by collocating on the exterior points, as follows:

$$[U^B(k)]_{2N\times 2N}\{t\}_{2N\times 1} = \{0\}, \tag{33}$$

$$[U^E(k)]_{a\times 2N}\{t\}_{2N\times 1} = \{0\}, \tag{34}$$

where the number of selected points $a\geq 1$ and E denote the exterior domain, respectively. To filter out spurious eigenvalues using the SVD technique, we can merge the two matrices in Eqs. (33) and (34) together to obtain an overdetermined system

$$[G(k)]_{(2N+a)\times 2N}\{t\}_{2N\times 1} = \{0\}, \tag{35}$$

where the $[G(k)]$ matrix with dimension $(2N+a)$ by $2N$ instead of $4N$ by $2N$ in Eq. (30), is derived from the $[U^B]$ an additional $[U^E]$ matrix as shown below

$$[G(k)]_{(2N+a)\times 2N} = \begin{bmatrix} U^B(k) \\ U^E(k) \end{bmatrix}_{(2N+a)\times 2N} \tag{36}$$

for the Dirichlet problem.

Even though the $[G(k)]$ matrix has dependent rows resulting from the degenerate boundary, the SVD technique can still be employed to find all the true eigenvalues since enough constraints are imbedded in the overdetermined matrix, $[G(k)]$. As for the true eigenvalues, the rank of the $[G(k)]$ matrix with dimension $(2N+a)$ by $2N$ must be at most $2N-1$ to have a nontrivial solution. As for the spurious eigenvalues, the rank must be $2N$ to obtain a trivial solution. Based on this criterion, the SVD technique can be employed to detect the true eigenvalues by checking whether or not the first minimum singular value, σ_1, is zero. Since discretization creates errors, very small values for σ_1, but not exactly zeros, will be obtained when k is near the critical wave number. In order to avoid determining the threshold for the zero numerically, a value of σ_1 closer to zero must be obtained using a smaller increment near the critical wave

985   J. Acoust. Soc. Am., Vol. 109, No. 3, March 2001

Chen *et al.*: Method for true and spurious eigensolutions   985

number, k. Such a value is confirmed to be a true eigenvalue. For the true eigenvalues with multiplicity of 2, we can consider the eigenvalues which make $\sigma_2 = 0$ and $\sigma_1 = 0$ at the same k value.

Since Eq. (36) is overdetemined, we will consider a linear algebra problem with more equations than unknowns

$$[\mathbf{A}]_{m \times n} \{\mathbf{x}\}_{n \times 1} = \{\mathbf{b}\}_{m \times 1}, \quad m > n, \tag{37}$$

where m is the number of equations, n is the number of unknowns, and $[\mathbf{A}]$ is the leading matrix, which can be decomposed into

$$[\mathbf{A}]_{m \times n} = [\mathbf{U}]_{m \times m} [\mathbf{\Sigma}]_{m \times n} [\mathbf{V}]^*_{n \times n}, \tag{38}$$

where $[\mathbf{U}]$ is a left unitary matrix constructed by the left singular vectors $(\mathbf{u}_1, \mathbf{u}_2, \mathbf{u}_3, \ldots, \mathbf{u}_m)$, $[\mathbf{\Sigma}]$ is a diagonal matrix which has singular values $\sigma_1, \sigma_2, \ldots,$ and σ_n allocated in a diagonal line as

$$[\mathbf{\Sigma}] = \begin{bmatrix} \sigma_n & \cdots & 0 \\ \vdots & \ddots & \vdots \\ 0 & \cdots & \sigma_1 \\ 0 & \cdots & 0 \\ 0 & \cdots & 0 \end{bmatrix}, \quad m > n, \tag{39}$$

in which $\sigma_n \geq \sigma_{n-1} \cdots \geq \sigma_1$ and $[\mathbf{V}]^*$ is the complex conjugate transpose of a right unitary matrix constructed by the right singular vectors $(\mathbf{v}_1, \mathbf{v}_2, \mathbf{v}_3, \ldots, \mathbf{v}_m)$. As we can see in Eq. (39), there exist at most n nonzero singular values. This means that we can find at most n linear independent equations in the system of equations. If we have p zero singular values $(0 \leq p \leq n)$, this means that the rank of the system of equations is equal to $n - p$. However, the singular value may be very close to zero numerically, resulting in rank deficiency. For a general eigenproblem as shown in this paper, the $[G(k)]$ matrix with dimension $(2N+a)$ by $2N$ will have a rank of $2N-1$ for the true eigenvalue with multiplicity 1 and $\sigma_1 = 0$, theoretically. For the true eigenvalues with multiplicity Q, the rank of $[G(k)]$ will be reduced to $2N-Q$ in which $\sigma_1, \sigma_2, \ldots,$ and σ_Q are zeros, theoretically. In other words, the matrix has a nullity of Q. In the case of spurious eigenvalues, the rank for the $[G(k)]$ matrix is $2N$, and the minimum singular value is not zero. Determining the eigenvalues of the system of equations has now been transformed into finding the values of k which make the rank of the leading coefficient matrix smaller than $2N$. This means that when $m = 2N+a, n = 2N$ and $\mathbf{b}_{(2N+a) \times 1} = \mathbf{0}$, the eigenvalues will make $p \geq 1$, such that the minimum singular values must be zero or very close to zero. Since we have employed the SVD technique to filter out the spurious eigenvalues, we can obtain the boundary mode by extracting the right unitary vector in SVD.

According to the definition of SVD, we have

$$[A] \mathbf{v}_p = \sigma_p \mathbf{u}_p, \quad p = 1, 2, 3, \ldots, n, \tag{40}$$

where $\mathbf{u}$ and $\mathbf{v}$ are the left and right unitary vectors, respectively. By choosing the qth zero singular value, σ_q, and substituting the qth right eigenvector, $\mathbf{v}_q$, into Eq. (40), we have
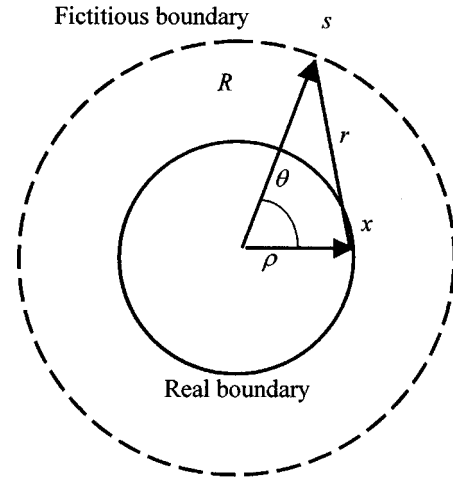

FIG. 3. The definitions of ρ, θ, R, and r.

$$[A] \mathbf{v}_q = 0 \mathbf{u}_q = \mathbf{0}, \quad q = 1, 2, 3 \ldots, Q. \tag{41}$$

According to Eq. (41), the nontrivial boundary mode is found to be the column vector of $\mathbf{v}_q$ in the right unitary matrix.

When we take all of the $2N+a$ equations into account, these apparently cause the rank of the leading coefficient matrix to be equal to $2N-1$ for the true eigenvalue with multiplicity 1. The boundary modes can be obtained from the $[V]$ matrix in Eq. (38) using SVD. Another advantage for using SVD is that it can determine the multiplicities for the true eigenvalues by finding the number of successive zeros in the singular values.

V. ANALYTICAL STUDY OF THE FAILURE POINTS IN THE CHEEF METHOD

In Refs. 27–29, the real-part U kernel can be expanded into

$$U(\mathbf{s}, \mathbf{x}) = \frac{\pi}{2} Y_0(kr) = \frac{\pi}{2} Y_0(k \sqrt{R^2 + \rho^2 - 2R\rho \cos \theta}), \tag{42}$$

where $\mathbf{x} = (\rho, \phi)$ and $\mathbf{s} = (R, \theta)$, ρ, r, R, and θ are shown in Fig. 3. Since $\mathbf{x}$ and $\mathbf{s}$ are on the boundaries of radius ρ and R, respectively, $U(\mathbf{s}, \mathbf{x})$ can be expanded into degenerate form as follows:

$$U(\mathbf{s}, \mathbf{x}) = \begin{cases} U(\theta, 0) = \sum_{n=-\infty}^{n=\infty} \frac{\pi}{2} Y_n(kR) J_n(k\rho) \cos(n\theta), & R > \rho, \\ U(\theta, 0) = \sum_{n=-\infty}^{n=\infty} \frac{\pi}{2} Y_n(k\rho) J_n(kR) \cos(n\theta), & R < \rho, \end{cases} \tag{43}$$

where the source point $\mathbf{s}$ and field point $\mathbf{x}(\phi = 0)$ in the two-point function is separated and $J_n(k\rho)$ is the nth order Bessel function of the first kind. Equation (43) can also be obtained through the addition theorem for the Hankel function. By superimposing $2N$ constant source distribution $\{\bar{t}\}$ along the fictitious boundary with radius R and collocating the $2N$ points on the boundary with radius ρ, we have

$$[U]\{\bar{t}\}=\begin{bmatrix} a_0 & a_1 & a_2 & \cdots & a_{2N-2} & a_{2N-1} \\ a_{2N-1} & a_0 & a_1 & \cdots & a_{2N-3} & a_{2N-2} \\ a_{2N-2} & a_{2N-1} & a_0 & \cdots & a_{2N-4} & a_{2N-3} \\ \vdots & \vdots & \vdots & \ddots & \vdots & \vdots \\ a_1 & a_2 & a_3 & \cdots & a_{2N-1} & a_0 \end{bmatrix}$$

$$\times \left\{ \begin{array}{c} \bar{t}_0 \\ \bar{t}_1 \\ \bar{t}_2 \\ \vdots \\ \bar{t}_{2N-1} \end{array} \right\} = \{0\} \qquad (44)$$

for the Dirichlet problem, where $\bar{t}_j$ is the fictitious density of single layer potential distributed on the boundary with radius R, and $[U]$ is the influence matrix with the elements shown below

$$a_m = \int_{(m-1/2)\Delta\theta}^{(m+1/2)\Delta\theta} U(\theta,0)R\,d\theta \approx U(\theta_m,0)R\Delta\theta,$$

$$m = 0,1,2,\ldots,2N-1, \qquad (45)$$

where $\Delta\theta = 2\pi/2N$ and $\theta_m = m\Delta\theta$.

The matrix $[U]$ in Eq. (44) is found to be a circulant since rotation the symmetry for the influence coefficients is considered. By introducing the following bases for the circulants $I, C_{2N}^1, C_{2N}^2, \ldots, C_{2N}^{2N-1}$, we can expand $[U]$ into

$$[U] = a_0 I + a_1 C_{2N}^1 + a_2 C_{2N}^2 + \cdots + a_{2N-1} C_{2N}^{2N-1}, \qquad (46)$$

where I is a unit matrix and

$$C_{2N} = \begin{bmatrix} 0 & 1 & 0 & \cdots & 0 & 0 \\ 0 & 0 & 1 & \cdots & 0 & 0 \\ \vdots & \vdots & \vdots & \ddots & \vdots & \vdots \\ 0 & 0 & 0 & \cdots & 0 & 1 \\ 1 & 0 & 0 & \cdots & 0 & 0 \end{bmatrix}_{2N \times 2N}. \qquad (47)$$

Based on the theory of circulants,[30] the spectral properties for the influence matrices, U, can be easily found as follows:

$$\lambda_l = a_0 + a_1 \alpha_l + a_2 \alpha_l^2 + \cdots + a_{2N-1} \alpha_l^{2N-1},$$

$$l = 0, \pm 1, \pm 2, \ldots, \pm(N-1), N, \qquad (48)$$

where λ_l and α_l are the eigenvalues for $[U]$ and $[C_{2N}]$, respectively. It is easily found that the eigenvalues for the circulants $[C_{2N}]$ are the roots for $z^{2N} = 1$ as shown below

$$\alpha_n = e^{i(2\pi n/2N)},$$

$$n = 0, \pm 1, \pm 2, \cdots, \pm(N-1), N$$

$$\text{or } n = 0,1,2,\ldots,2N-1, \qquad (49)$$

and the eigenvectors are

$$\{\phi_n\} = \left\{ \begin{array}{c} 1 \\ \alpha_n \\ \alpha_n^2 \\ \alpha_n^3 \\ \vdots \\ \alpha_n^{2N-1} \end{array} \right\}. \qquad (50)$$

Substituting Eq. (49) into Eq. (48), we have

$$\lambda_l = \sum_{m=0}^{2N-1} a_m \alpha_l^m = \sum_{m=0}^{2N-1} a_m e^{i(2\pi/2N)ml}$$

$$l = 0, \pm 1, \pm 2, \cdots, \pm(N-1), N. \qquad (51)$$

According to the definition for a_m in Eq. (45), we have

$$a_m = a_{2N-m}, \quad m = 0,1,2,\ldots,2N-1. \qquad (52)$$

Substituting Eq. (52) into Eq. (51), we have

$$\lambda_l = a_0 + (-1)^l a_N + \sum_{m=1}^{N-1} (\alpha_l^m + \alpha_l^{2N-m}) a_m$$

$$= \sum_{m=0}^{2N-1} \cos(ml\Delta\theta) a_m. \qquad (53)$$

Substituting Eq. (45) into Eq. (53), we have

$$\lambda_l \approx \sum_{m=0}^{2N-1} \cos(ml\Delta\theta) U(m\Delta\theta,0)R\Delta\theta$$

$$= \int_0^{2\pi} \cos(l\theta) U(\theta,0)R\,d\theta, \qquad (54)$$

as N approaches infinity. Equation (54) reduces to

$$\lambda_l = \int_0^{2\pi} \cos(l\theta) \sum_{m=-\infty}^{\infty} \frac{\pi}{2} Y_m(kR) J_m(k\rho) \cos m\theta R\,d\theta$$

$$= \pi^2 R Y_l(kR) J_l(k\rho). \qquad (55)$$

Since the wave number k is imbedded in each element of the $[U]$ matrix, the eigenvalues for $[U]$ are also functions of k. Finding the eigenvalues for the Helmholtz equation or finding the zeros for the determinant of $[U]$ is equal to finding the zeros for the multiplication of all of the eigenvalues of $[U]$. Based on the following equation:
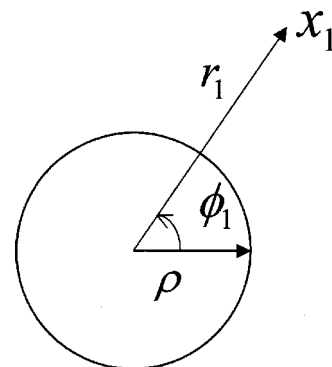

FIG. 4. One sample point.

TABLE I. Zeros of Bessel function for $J_n(k)$ and $Y_n(k)$.

	1	2	3	4	5
$J_0(k)=0$	2.404 8	5.520 1	8.653 7	11.791 5	14.930 9
$J_1(k)=0$	3.831 71	7.015 59	10.173 46	13.323 7	16.4706
$J_2(k)=0$	5.135 6	8.417 2	11.619 8	14.796 0	17.959 8
$J_3(k)=0$	6.380 16	9.760 12	13.015 2	16.223 46	19.409 41
$J_4(k)=0$	7.588 34	11.064 7	14.372 5	17.616 0	20.826 9
$J_5(k)=0$	8.771 48	12.338 6	15.700 2	18.980 1	22.217 8
$Y_0(k)=0$	0.893 58	3.957 68	7.086 05	10.222 34	13.361 10
$Y_1(k)=0$	2.197 14	5.429 68	8.596 01	11.749 15	14.897 44
$Y_2(k)=0$	3.384 24	6.793 81	10.023 48	13.209 99	16.378 97
$Y_3(k)=0$	4.527 02	8.097 75	11.396 47	14.623 07	17.818 45
$Y_4(k)=0$	5.645 15	9.361 62	12.730 1	15.999 6	19.224 4
$Y_5(k)=0$	6.747 18	10.597 2	14.033 8	17.347 1	20.602 9

$$\det[U]=\lambda_0\lambda_N(\lambda_1\lambda_2\cdots\lambda_{N-1})(\lambda_{-1}\lambda_{-2}\cdots\lambda_{-(N-1)}),\tag{56}$$

the possible eigenvalues (true or spurious) occur at

$$Y_l(kR)J_l(k\rho)=0, \quad l=0,\pm 1,\pm 2,\cdots,\pm(N-1),N.\tag{57}$$

The k values satisfying Eq. (57) may be spurious eigenvalue or true eigenvalue. Here, we adopted the CHIEF method concept to filter out the spurious eigenvalues.

If we adopt one exterior point (r_1,ϕ_1), where $r_1>\rho$ as shown in Fig. 4, we have

$$0=\int_B U(s,x)t(s)dB(s)=[w_1^T]\{t\},\tag{58}$$

where $[w_1^T]=(w_1^1,w_1^2,w_1^3,\ldots,w_1^{2N})$ is the row vector of the influence matrix by collocating the exterior point x_1. Combining Eq. (44) and Eq. (58), we obtain an overdetermined system

$$\begin{bmatrix} U(k) \\ w_1^T(k) \end{bmatrix}\{t\}=\{0\},\tag{59}$$

where $\{t\}=\{1,e^{in\Delta\theta},e^{in2\Delta\theta},\ldots,e^{in(2N-1)\Delta\theta}\}^T$.

The additional constraint $[w_1^T]\{t\}=0$ provide the discriminant, $\triangle$, to be

$$\triangle=[w_1^T]\{t\}=\pi^2 r_1 Y_n(kr_1)J_n(k\rho)e^{in\phi_1}=0.\tag{60}$$

For the single spurious eigenvalues $k_{0,m}^s$, we have $Y_0(k_{0,m}^s)=0$, where the superscript s denotes the spurious eigenvalues and $k_{0,m}$ denotes the mth zeros for the Y_0 function [zeros of the Bessel function for $J_n(k)$ and $Y_n(k)$ are shown in Table I]. If the selected exterior point (r_1,ϕ_1), satisfies

$$k_{0,m}^s r_1=k_{0,p} \quad (m<p),\tag{61}$$

where $k_{0,p}$ denotes the pth zeros for the Y_0 function, then the spurious eigenvalues $k_{0,m}^s$, cannot be filtered out. For the double spurious eigenvalues $k_{n,m}^s$, we have $Y_n(k_{n,m}^s)=0$, $n>0$. If the selected exterior point (r_1,ϕ_1), satisfies

$$k_{n,m}^s r_1=k_{n,p} \quad (m<p),\tag{62}$$

then the spurious eigenvalues $k_{n,m}^s$, cannot be filtered out. The possible failure positions for r_1 are shown in Table II. When the spurious eigenvalues are double roots, rank reduces by 2. One point provides at most one constraint. One point cannot filter out the double spurious roots, so an additional independent equation is required by adding one more point.

If we adopt another exterior point (r_2,ϕ_2) with a radial distance $r_2>\rho$ as shown in Fig. 5, and combine with Eq. (59), we have

$$\begin{bmatrix} U(k) \\ w_1^T(k) \\ w_2^T(k) \end{bmatrix}\{t\}=\{0\},\tag{63}$$

where $[w_2^T]=(w_2^1,w_2^2,w_2^3,\ldots w_2^{2N})$ is the row vector of the influence matrix by collocating the exterior point x_2. When the spurious eigenvalues are double roots, we have

$$\begin{bmatrix} w_1^T(k) \\ w_2^T(k) \end{bmatrix}\{t\}=\begin{bmatrix} w_1^T \\ w_2^T \end{bmatrix}\{\alpha t_1+\beta t_2\}=\begin{bmatrix} w_1^T t_1 & w_1^T t_2 \\ w_2^T t_1 & w_2^T t_2 \end{bmatrix}\begin{Bmatrix} \alpha \\ \beta \end{Bmatrix},\tag{64}$$

where $\{t_1\}=\{1,e^{in\Delta\theta},e^{in2\Delta\theta},\ldots,e^{in(2N-1)\Delta\theta}\}^T$ and $\{t_2\}=\{1,e^{-in\Delta\theta},e^{-in2\Delta\theta},\ldots,e^{-in(2N-1)\Delta\theta}\}^T$ are two independent boundary modes, α and β are two constants, and

$$w_1^T t_1^T=\pi^2 r_1 Y_n(kr_1)J_n(k\rho)e^{in\phi_1},$$
$$w_1^T t_2^T=\pi^2 r_1 Y_n(kr_1)J_n(k\rho)e^{-in\phi_1},$$
$$w_2^T t_1^T=\pi^2 r_2 Y_n(kr_2)J_n(k\rho)e^{in\phi_2},$$
$$w_2^T t_2^T=\pi^2 r_2 Y_n(kr_2)J_n(k\rho)e^{-in\phi_2}.$$

Since the spurious double roots make the rank less than 2, the additional two points must provide independent constraints, as follows:

$$\begin{bmatrix} \pi^2 r_1 Y_n(kr_1)J_n(k\rho)e^{in\phi_1} & \pi^2 r_1 Y_n(kr_1)J_n(k\rho)e^{-in\phi_1} \\ \pi^2 r_2 Y_n(kr_2)J_n(k\rho)e^{in\phi_2} & \pi^2 r_2 Y_n(kr_2)J_n(k\rho)e^{-in\phi_2} \end{bmatrix}\begin{bmatrix} \alpha \\ \beta \end{bmatrix}=0.\tag{65}$$

TABLE II. The failure points with difference radial circular.

Failure point				
$Y_{0,1}$	3.96/0.89=4.429	7.09/0.89=7.97	10.22/0.89=11.48	13.36/0.89=15.01
$Y_{0,2}$	7.09/3.96=1.79	10.22/3.96=2.58	13.36/3.96=3.37	
$Y_{0,3}$	10.22/7.09=1.44	13.36/7.09=1.88		
$Y_{1,1}$	5.43/2.2=2.47	8.6/2.2=3.91	11.75/2.2=5.34	14.9/2.2=6.77
$Y_{1,2}$	8.6/5.43=1.58	11.75/5.43=2.16	14.9/5.43=2.74	
$Y_{1,3}$	11.75/8.6=1.37	14.9/8.6=1.73		
$Y_{2,1}$	6.79/3.38=2.007	10.02/3.38=2.96	13.21/3.38=3.91	16.38/3.38=4.85
$Y_{2,2}$	10.02/6.79=1.48	13.21/6.79=1.94	16.38/6.79=2.41	
$Y_{2,3}$	13.21/10.02=1.32	16.38/10.02=1.63		
$Y_{3,1}$	8.1/4.53=1.79	11.4/4.53=2.52	14.62/4.53=3.23	17.82/4.53=3.93
$Y_{3,2}$	11.4/8.1=1.41	14.62/8.1=1.80	17.82/8.1=2.2	
$Y_{3,3}$	14.62/11.4=1.28	17.82/11.4=1.56		
$Y_{4,1}$	9.36/5.64=1.66	12.73/5.64=2.26	16/5.64=2.84	19.22/5.64=3.41
$Y_{4,2}$	12.73/9.36=1.36	16.0/9.36=1.71	19.22/9.36=2.05	
$Y_{4,3}$	16.0/12.73=1.26	19.22/12.73=1.51		
$Y_{5,1}$	10.6/6.75=1.57	14.03/6.75=2.08	17.35/6.75=2.57	20.6/6.75=3.05
$Y_{5,2}$	14.03/10.6=1.32	17.35/10.6=1.64	20.6/10.6=1.94	
$Y_{5,3}$	17.35/14.03=1.24	20.6/14.03=1.47		

If they are dependent, we have

$$\triangle = \det \begin{vmatrix} \pi^2 r_1 Y_n(kr_1)J_n(k\rho)e^{in\phi_1} & \pi^2 r_1 Y_n(kr_1)J_n(k\rho)e^{-in\phi_1} \\ \pi^2 r_2 Y_n(kr_2)J_n(k\rho)e^{in\phi_2} & \pi^2 r_2 Y_n(kr_2)J_n(k\rho)e^{-in\phi_2} \end{vmatrix}$$

$$= r_1 r_2 Y_n(kr_1)Y_n(kr_2)J_n(k\rho)J_n(k\rho)(e^{in(\phi_1-\phi_2)} - e^{-in(\phi_1-\phi_2)}) = i2r_1 r_2 Y_n(kr_1)Y_n(kr_2)J_n(k\rho)J_n(k\rho)\sin(n\phi) = 0,$$

$$(66)$$

where $\phi = \phi_1 - \phi_2$ indicates the intersecting angle between the two exterior points. The discriminant $\triangle$ indicates

(1) If the two points with the intersection angle ϕ produce $\sin(n\phi) = \sin(\pi) = 0$, i.e., $\phi = \pi/n$, we will fail to filter out the double spurious roots for Y_n, $n \geq 1$.
(2) If the two points produce $Y_n(kr_1) = 0$ or $Y_n(kr_2) = 0$, $n = 1,2,3,\ldots$, then we will fail to filter out the double spurious root of Y_n.
(3) No more than two points are needed if the points are properly chosen.

For the Neumann problem
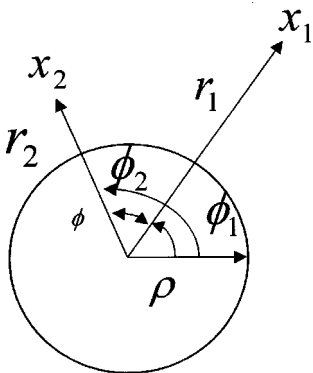
FIG. 5. Two sample points.

$$[T]\{\bar{u}\} = \begin{bmatrix} b_0 & b_1 & b_2 & \cdots & b_{2N-2} & b_{2N-1} \\ b_{2N-1} & b_0 & b_1 & \cdots & b_{2N-3} & b_{2N-2} \\ b_{2N-2} & b_{2N-1} & b_0 & \cdots & b_{2N-4} & b_{2N-3} \\ \vdots & \vdots & \vdots & \ddots & \vdots & \vdots \\ b_1 & b_2 & b_3 & \cdots & b_{2N-1} & b_0 \end{bmatrix}$$

$$\times \left\{ \begin{array}{c} \bar{u}_0 \\ \bar{u}_1 \\ \bar{u}_2 \\ \vdots \\ \bar{u}_{2N-1} \end{array} \right\} = 0, \quad (67)$$

where $\bar{u}_j$ is the fictitious density of single layer potential distributed on the boundary with radius R, and the boundary mode for $\{\bar{u}\}$ is

$$\{\bar{u}\} = \{1, e^{in\Delta\theta}, e^{in2\Delta\theta}, \cdots, e^{in(2N-1)\Delta\theta}\}^T \quad (68)$$

where n denotes the nth boundary mode. The matrix $[T]$ is the influence matrix with the elements shown below

$$b_m = \int_{(m-1/2)\Delta\theta}^{(m+1/2)\Delta\theta} T(\theta,0)R\,d\theta \approx T(\theta_m,0)R\Delta\theta,$$
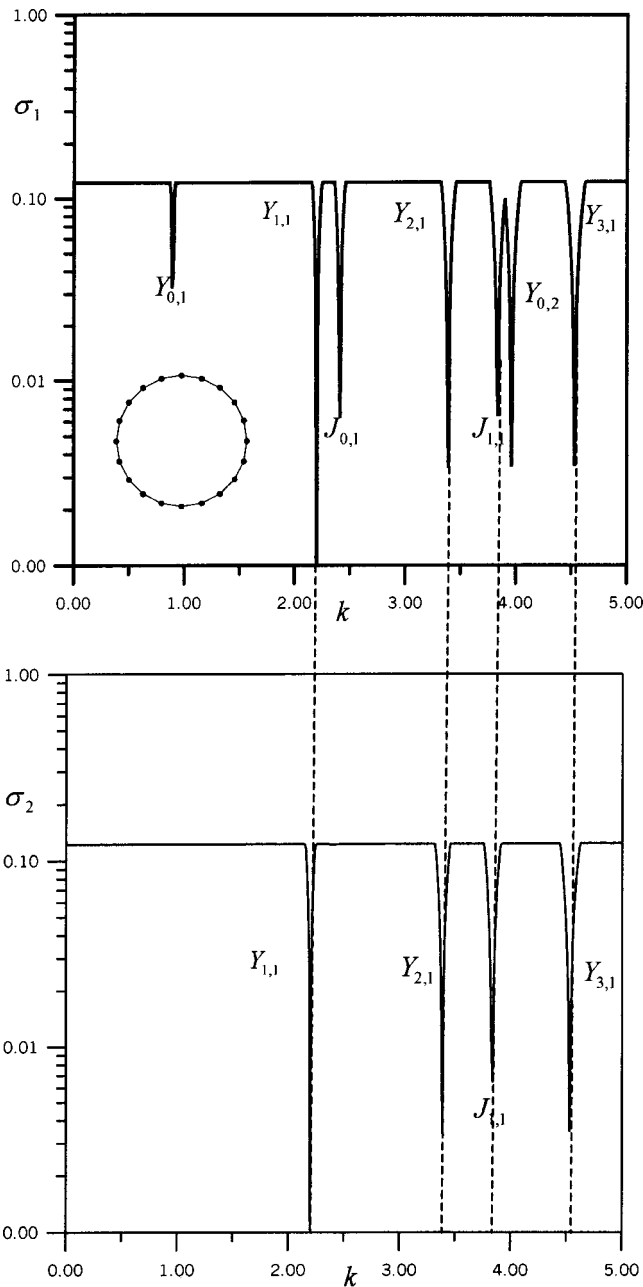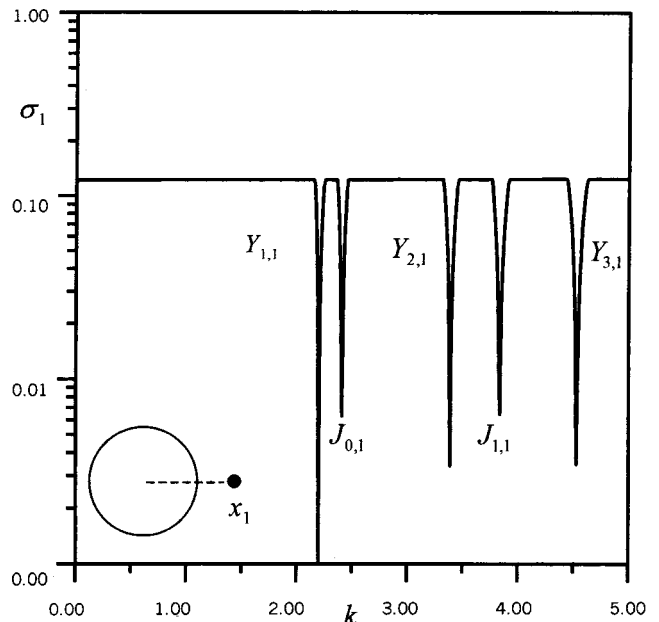
$$m = 0,1,2,\ldots,2N-1, \quad (69)$$

FIG. 7. One sample point $x_1(1.5,0)$, σ_1 vs k using the real-part UT equation.

$$\mu_l = b_0 + b_1 \alpha_l + b_2 \alpha_l^2 + \cdots + b_{2N-1} \alpha_l^{2N-1},$$

$$l = 0, \pm 1, \pm 2, \cdots, \pm (N-1), N, \qquad (72)$$

where μ_l and α_l are the eigenvalues for $[T]$ and $[C_{2N}]$, respectively.

We have

$$\mu_l = \sum_{m=0}^{2N-1} b_m \alpha_l^m$$

$$= \sum_{m=0}^{2N-1} b_m e^{i(2\pi/2N)ml},$$

$$l = 0, \pm 1, \pm 2, \cdots, \pm (N-1), N. \qquad (73)$$
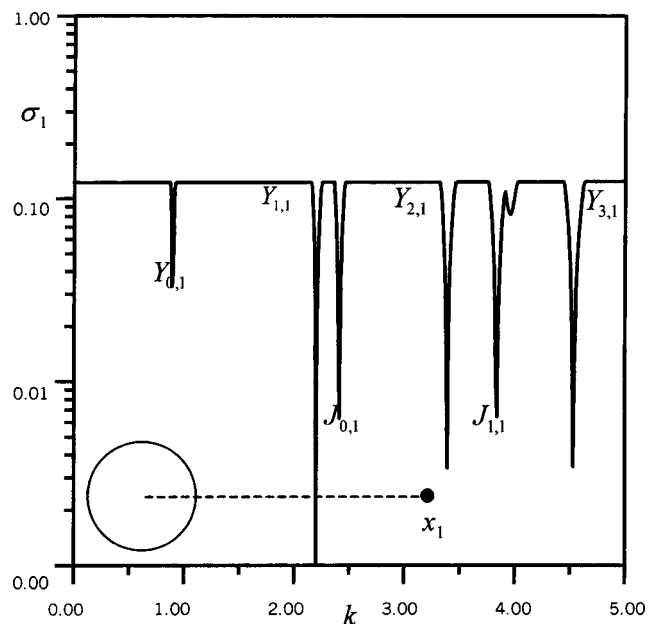
FIG. 8. One sample point $x_1(4.429,0)$, σ_1 vs k using the real-part UT equation.

FIG. 6. The first and second minimum singular values σ_1 and σ_2 vs k of a circular using the real-part UT equation subject to Dirichlet boundary conditions and boundary mesh.

where $\Delta \theta = 2\pi/2N$ and $\theta_m = m\Delta \theta$, $T(\mathbf{s},\mathbf{x})$ can be expanded into

$$T(\mathbf{s},\mathbf{x}) = T(\theta,0)$$

$$= \sum_{n=-\infty}^{\infty} \frac{\pi}{2} Y_n(kR) J_n'(k\rho) \cos(n\theta), \quad R > \rho. \quad (70)$$

The matrix $[T]$ in Eq. (67) is a circulant since rotation symmetry for the influence coefficients are considered. We can expand $[T]$ into

$$[T] = b_0 I + b_1 C_{2N}^1 + b_2 C_{2N}^2 + \cdots + b_{2N-1} C_{2N}^{2N-1}. \quad (71)$$

Based on the theory of circulants, the spectral properties for the influence matrix, $[T]$, can be found as follows:

FIG. 9. The spurious eigenvalue radiation mode of a circular cavity for the Dirichlet problem with $k_s = 0.894$.

FIG. 11. The spurious eigenvalue radiation mode of a circular cavity for the Dirichlet problem with $k_s = 3.384$.

According to the definition for b_m in Eq. (69), we have

$$b_m = b_{2N-m}, \quad m = 0,1,2,\ldots,2N-1. \tag{74}$$

Substituting Eq. (74) into Eq. (73), we have

$$\mu_l = b_0 + (-1)^l b_N + \sum_{m=1}^{N-1} (\alpha_l^m + \alpha_l^{2N-m}) b_m$$

$$= \sum_{m=0}^{2N-1} \cos(ml\Delta\theta) b_m. \tag{75}$$

Substituting Eq. (69) into Eq. (75), we have

$$\mu_l \approx \sum_{m=0}^{2N-1} \cos(ml\Delta\theta) T(m\Delta\theta,0) R\Delta\theta$$

$$= \int_0^{2\pi} \cos(l\theta) T(\theta,0) R\, d\theta, \tag{76}$$

as N approaches infinity. Equation (76) reduces to

$$\mu_l = \int_0^{2\pi} \cos(l\theta) \sum_{m=-\infty}^{\infty} \frac{\pi}{2} Y_m(kR) J_m'(k\rho) \cos m\theta R\, d\theta$$

$$= \pi^2 R Y_l(kR) J_l'(k\rho). \tag{77}$$
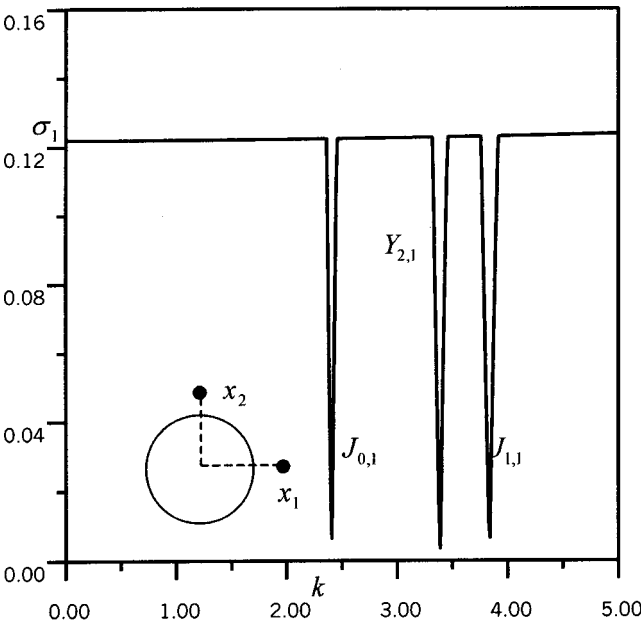
FIG. 10. Two sample points $x_1(1.5,0)$ and $x_2(1.5,\pi/2)$, σ_1 vs k using the real-part UT equation.
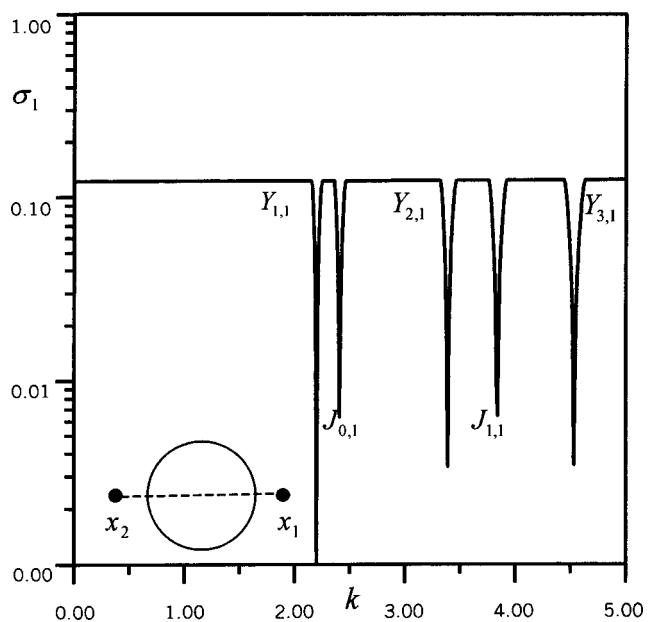
FIG. 12. Two sample points $x_1(1.5,0)$ and $x_2(1.5,\pi)$, σ_1 vs k using the real-part UT equation.
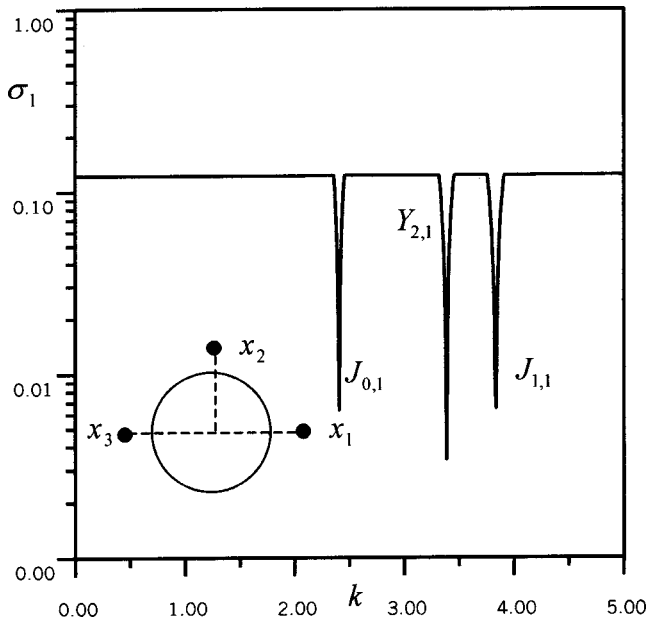
FIG. 13. Three sample points $x_1(1.5,0)$, $x_2(1.5,\pi/2)$, and $x_3(1.5,\pi)$, σ_1 vs k using the real-part UT equation.
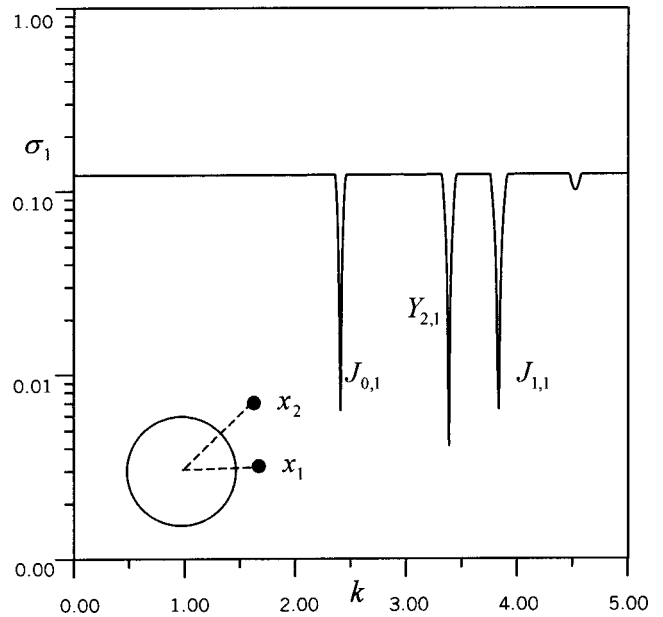
FIG. 15. Two sample points $x_1(2.007,\pi/4)$ and $x_2(1.4,0)$, σ_1 vs k using the real-part UT equation.

Since the wave number k is imbedded in each element of the $[T]$ matrix, the eigenvalues for $[T]$ are also a function of k. Finding the eigenvalues for the Helmholtz equation or finding the zeros for the determinant of $[T]$ is equal to finding the zeros for multiplication of all the eigenvalues of $[T]$. Based on the following equation:

$$\det[T] = \mu_0 \mu_N (\mu_1 \mu_2 \cdots \mu_{N-1})(\mu_{-1} \mu_{-2} \cdots \mu_{-(N-1)}), \quad (78)$$

the possible eigenvalues (true or spurious) occur at

$$Y_l(kR)J_l'(k\rho) = 0, \quad l = 0, \pm 1, \pm 2, \cdots, \pm(N-1), N. \quad (79)$$

The values satisfying Eq. (79) may be spurious eigenvalues or true eigenvalues. Similarly, we adopted the same method to filter out the spurious eigenvalues.

If we adopt one exterior point (r_1, ϕ_1), where $r_1 > \rho$ as shown in Fig. 4, for exterior point

$$0 = \int_B T(s,x)t(s)dB(s) = [v_1^T]\{u\}, \quad (80)$$

where $[v_1^T] = (v_1^1, v_1^2, v_1^3, \ldots, v_1^{2N})$ is the row vector of the influence matrix by collocating the exterior point x_1. Com-
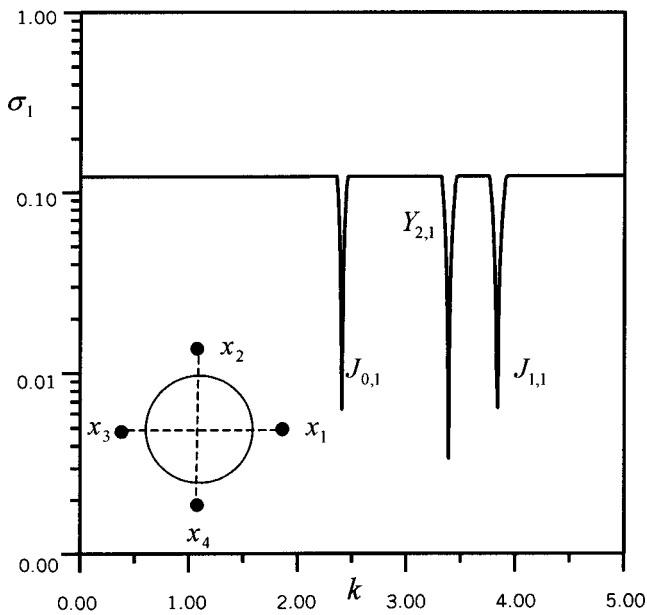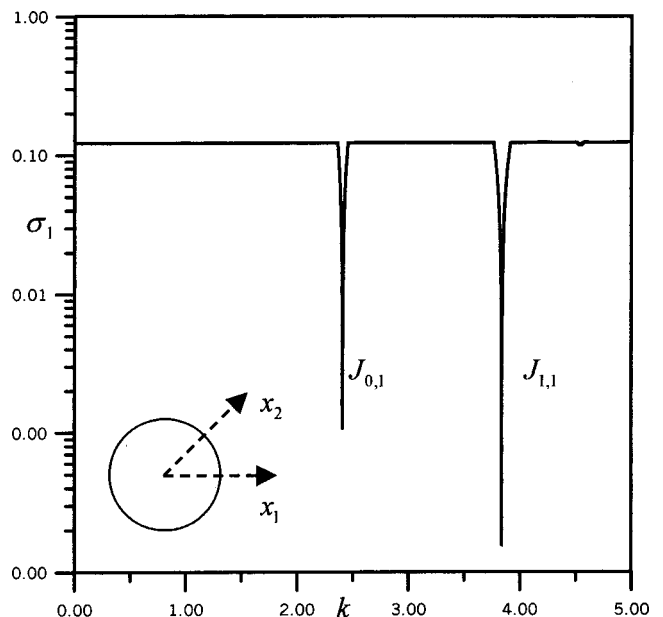

FIG. 14. Four sample points $x_1(1.5,0)$, $x_2(1.5,\pi/2)$, $x_3(1.5,\pi)$, and $x_4(1.5,3\pi/2)$, vs k using the real-part UT equation.

FIG. 16. Two sample points $x_1(1.5,0)$ and $x_2(1.5,\pi/4)$, σ_1 vs k using the real-part.
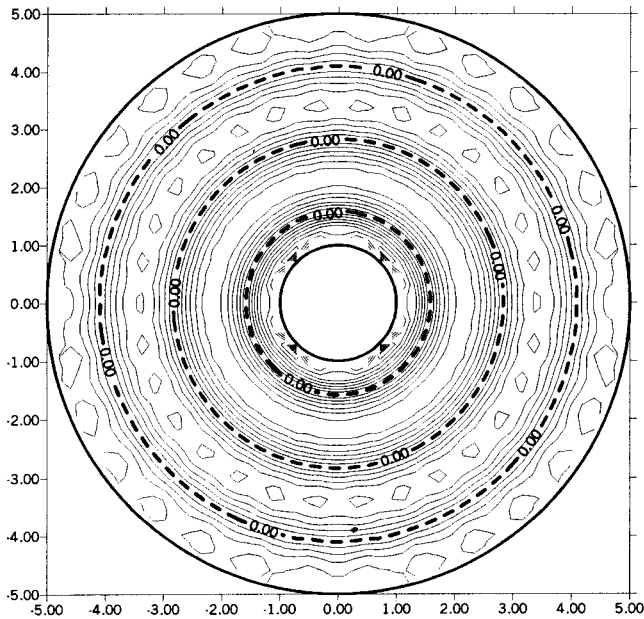
FIG. 17. The true eigenvalue radiation mode of a circular cavity for the Dirichlet problem with $k_T = 2.405$.

bining Eq. (67) and Eq. (80), we obtain an overdeterminate system

$$
\begin{bmatrix} T(k) \\ v_1^T(k) \end{bmatrix} \{u\} = \{0\}, \tag{81}
$$

where $\{u\} = \{1, e^{in\Delta\theta}, e^{in2\Delta\theta}, \ldots, e^{in(2N-1)\Delta\theta}\}^T$.

The additional constraint $[v_1^T]\{u\} = 0$ provides the discriminant, $\triangle$, to be

$$
\triangle = [v_1^T]\{u\} = \pi^2 r_1 Y_n(kr_1) J_n'(k\rho) e^{in\phi_1} = 0. \tag{82}
$$
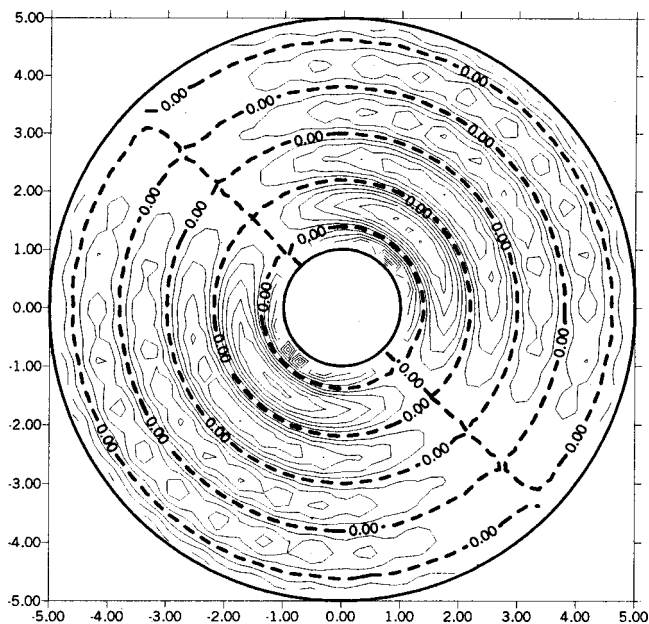
FIG. 18. The true eigenvalue radiation mode of a circular cavity for the Dirichlet problem with $k_T = 3.832$.
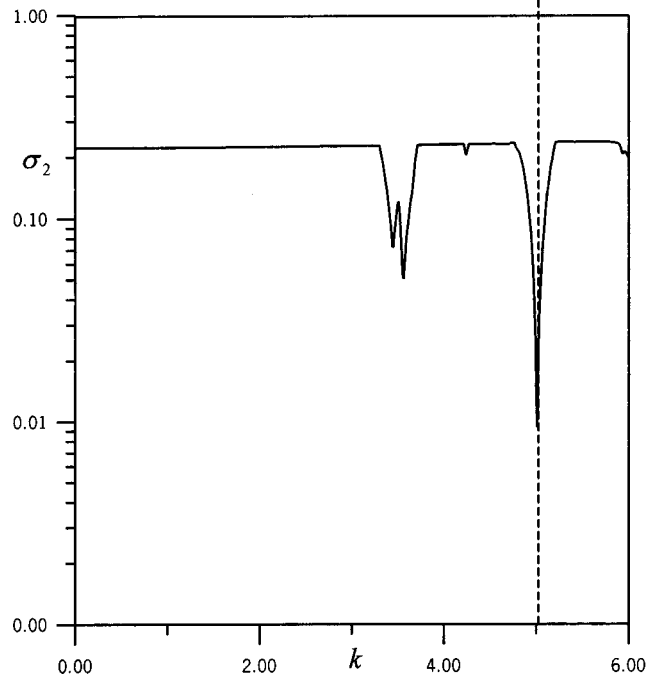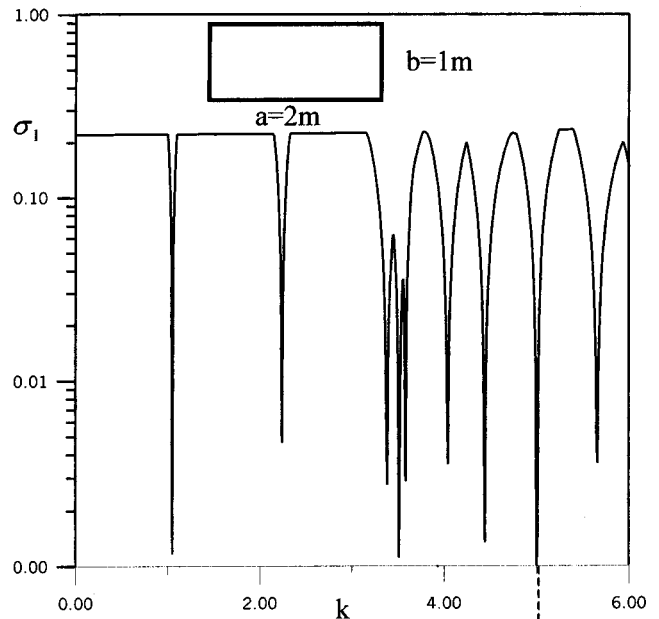
FIG. 19. The first and second minimum singular values σ_1 and σ_2 vs k of a rectangle using the real-part UT equation subject to Dirichlet boundary conditions with size 2 m×1 m.

It is similar to Eq. (60), it can filter out a single root only.

If we adopt another exterior point (r_2, ϕ_2) with a radial distance $r_2 > \rho$ as shown in Fig. 5, and combine with Eq. (81), we have

$$
\begin{bmatrix} T(k) \\ v_1^T(k) \\ v_2^T(k) \end{bmatrix} \{u\} = \{0\}, \tag{83}
$$

where $[v_2^T] = (v_2^1, v_2^2, v_2^3, \ldots, v_2^{2N})$ is the row vector of the influence matrix by collocating the exterior point x_2. When the spurious eigenvalues are double roots, we have
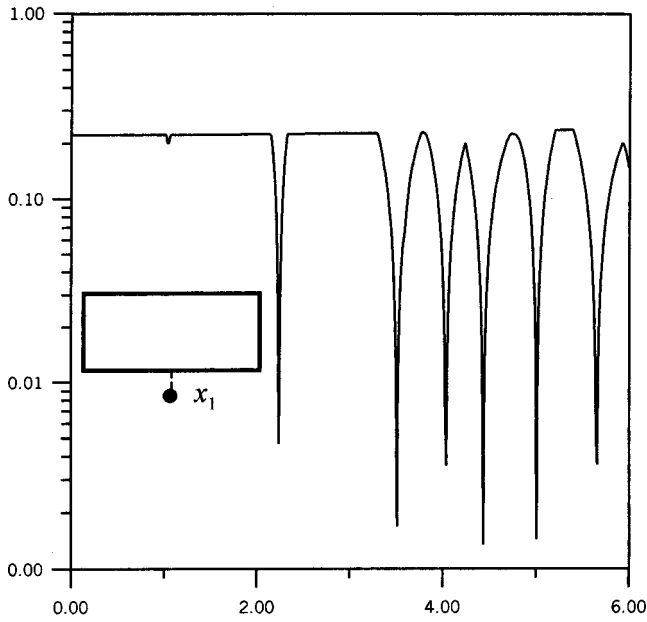
FIG. 20. One sample point $x_1(1.0, -0.25)$, σ_1 vs k using the real-part UT equation.

$$\begin{bmatrix} v_1^T(k) \\ v_2^T(k) \end{bmatrix} \{u\} = \begin{bmatrix} v_1^T \\ v_2^T \end{bmatrix} \{\alpha u_1 + \beta u_2\} = \begin{bmatrix} v_1^T u_1 & v_1^T u_2 \\ v_2^T u_1 & v_2^T u_2 \end{bmatrix} \begin{Bmatrix} \alpha \\ \beta \end{Bmatrix},$$
(84)

where $\{u_1\} = \{1, e^{in\Delta\theta}, e^{in2\Delta\theta}, \ldots, e^{in(2N-1)\Delta\theta}\}^T$ and $\{u_2\} = \{1, e^{-in\Delta\theta}, e^{-in2\Delta\theta}, \ldots, e^{-in(2N-1)\Delta\theta}\}^T$ are two independent boundary modes, α and β are constants, and

$$v_1^T u_1^T = \pi^2 r_1 Y_n(kr_1) J_n'(k\rho) e^{in\phi_1},$$

$$v_1^T u_2^T = \pi^2 r_1 Y_n(kr_1) J_n'(k\rho) e^{-in\phi_1},$$

$$v_2^T u_1^T = \pi^2 r_2 Y_n(kr_2) J_n'(k\rho) e^{in\phi_2},$$

FIG. 22. The spurious eigenvalue radiation mode of a rectangle for the Dirichlet problem with $k_s = 4.02$.

$$v_2^T u_2^T = \pi^2 r_2 Y_n(kr_2) J_n'(k\rho) e^{-in\phi_2}.$$

Since the spurious double roots make the rank less than 2, the additional two points must provide independent constraints, as follows

$$\begin{bmatrix} \pi^2 r_1 Y_n(kr_1) J_n'(k\rho) e^{in\phi_1} & \pi^2 r_1 Y_n(kr_1) J_n'(k\rho) e^{-in\phi_1} \\ \pi^2 r_2 Y_n(kr_2) J_n'(k\rho) e^{in\phi_2} & \pi^2 r_2 Y_n(kr_2) J_n'(k\rho) e^{-in\phi_2} \end{bmatrix}$$

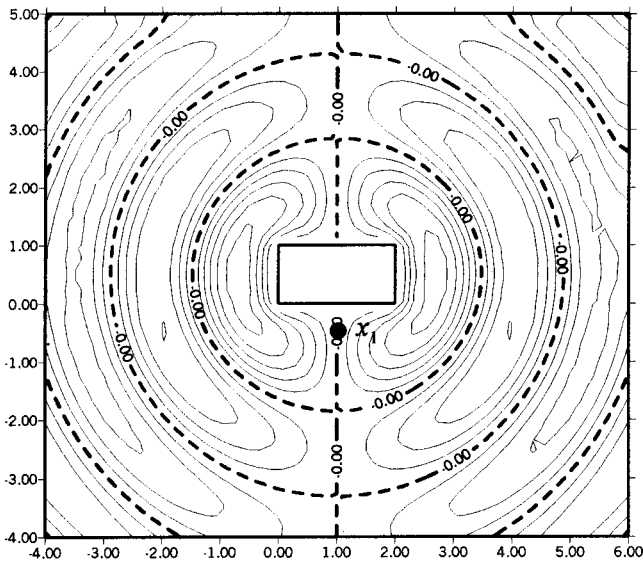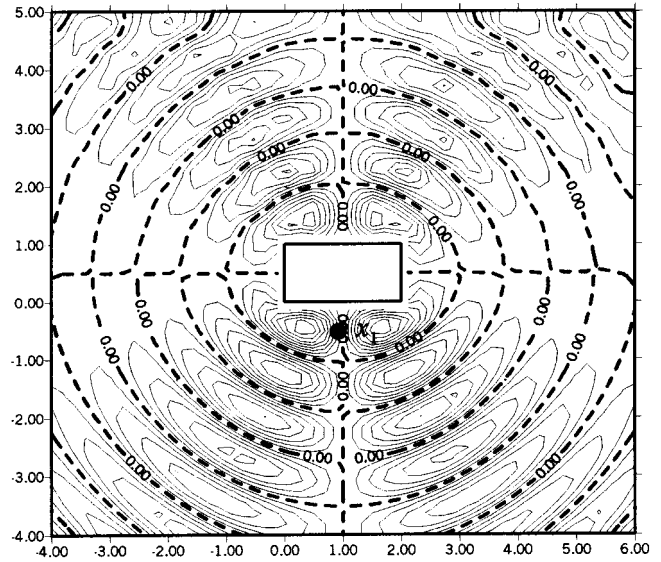$$\times \begin{bmatrix} \alpha \\ \beta \end{bmatrix} = 0.$$
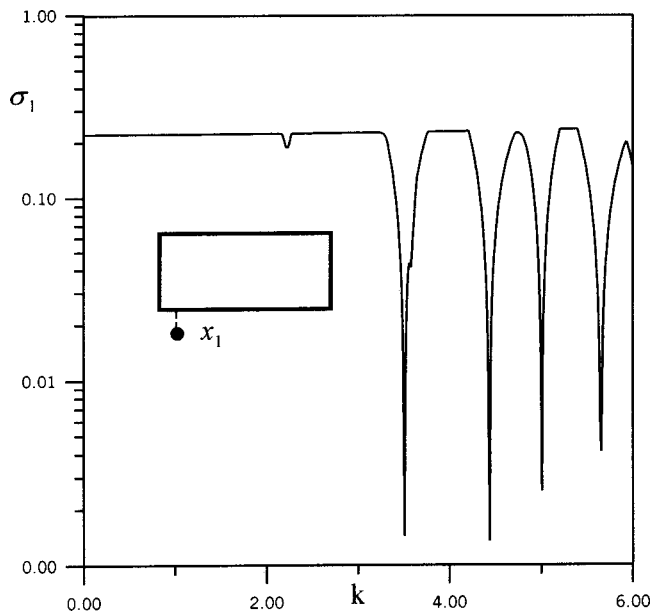(85)

If they are dependent, we have

FIG. 21. The spurious eigenvalue radiation mode of a rectangle for the Dirichlet problem with $k_s = 2.23$.

FIG. 23. One sample point $x_1(0.25, -0.25)$, σ_1 vs k using the real-part UT equation.

$$\triangle = \det \begin{vmatrix} \pi^2 r_1 Y_n(kr_1)J_n'(k\rho)e^{in\phi_1} & \pi^2 r_1 Y_n(kr_1)J_n'(k\rho)e^{-in\phi_1} \\ \pi^2 r_2 Y_n(kr_2)J_n'(k\rho)e^{in\phi_2} & \pi^2 r_2 Y_n(kr_2)J_n'(k\rho)e^{-in\phi_2} \end{vmatrix}$$

$$= r_1 r_2 Y_n(kr_1)Y_n(kr_2)J_n'(k\rho)J_n'(k\rho)(e^{in(\phi_1-\phi_2)} - e^{-in(\phi_1-\phi_2)}) = r_1 r_2 Y_n(kr_1)Y_n(kr_2)J_n'(k\rho)J_n'(k\rho)2i\sin(n\phi) = 0,$$

$$(86)$$

where $\phi = \phi_1 - \phi_2$ indicates the intersecting angle between the two exterior points. Similarly, the discriminant $\triangle$ can justify whether the selected point is effective or not. It can filter out a double root. It was found that the spurious eigenvalues of an interior problem are dependent on the chosen method, i.e., singular integral equation results in the spurious eigenvalues at $Y_n(k\rho) = 0$, and independent of boundary condition (Dirichlet or Neumann).

VI. NUMERICAL EXAMPLES

For the numerical experiment, we considered a circular cavity with radius 1 m subjected to the Dirichlet boundary condition to check the validity of the CHEEF method. Furthermore, in order to extend to the general geometry problem using the CHEEF method, we used a rectangular cavity subjected to the Dirichlet boundary condition to demonstrate the generality.

Sixty elements were adopted in the boundary element mesh for a circular domain. Figure 6 shows the first minimum singular value, σ_1, vs k where the true and spurious eigenvalues are obtained if only real-part UT is used. In the range of $0 < k < 5$, we have two true eigenvalues $[J_{0,1}(2.405)$ and $J_{1,1}(3.832)]$ and five spurious eigenvalues $[Y_{0,1}(0.894)$, $Y_{1,1}(2.197)$, $Y_{2,1}(3.384)$, $Y_{0,2}(3.958)$, and $Y_{3,1}(4.527)]$.[11] Figure 6 also indicates the second minimum singular value, σ_2, vs k where the true and spurious double roots can be

obtained, when σ_1 and σ_2 are both zeros at the same k value. Figure 7 shows σ_1 vs k by additionally considering Eq. (58) for collocating one exterior point, $\mathbf{x}_1$, with radius $r_1 = 1.5$ m, $\phi_1 = 0$. This treatment can filter out the spurious roots of $Y_{0,1}$ and $Y_{0,2}$ as expected in the analytical derivation. If the collocating exterior point is located at the circular boundary with radius $r_1 = k_{0,2}/k_{0,1} = 3.590/0.894 = 4.429$ as described in Eq. (61), which is on the nodal line of the radiation mode of $Y_{0,1}$, then the spurious eigenvalue of $Y_{0,1}$ cannot be filtered out as shown in Fig. 8. The spurious radiation mode of $Y_{0,1}$ is shown in Fig. 9.

If the additional two points $\mathbf{x}_1(r_1 = 1.5, \phi_1 = 0)$ and $\mathbf{x}_2(r_2 = 1.5, \phi_2 = \pi/2)$ with intersecting angle of $\phi = \pi/2$ are selected, then the spurious root of $Y_{2,1}$ cannot be filtered out as shown in Fig. 10, since $\sin 2\phi = 0$. The spurious radiation mode of $Y_{2,1}$ is shown in Fig. 11. Similarly, in both positions $\mathbf{x}_1$ and $\mathbf{x}_2$ with intersecting angle π, only the spurious eigenvalue $Y_{0,1}$ and $Y_{0,2}$ can be filtered out as shown in Fig. 12. Figure 13 and Fig. 14 are the results by adopting three $[(\mathbf{x}_1(r_1 = 1.5, \phi_1 = 0), \mathbf{x}_2(r_2 = 1.5, \phi_2 = \pi/2), \mathbf{x}_3(r_3 = 1.5, \phi_3 = \pi)]$ and four $[(\mathbf{x}_1(r_1 = 1.5, \phi_1 = 0), \mathbf{x}_2(r_2 = 1.5, \phi_2 = \pi/2), \mathbf{x}_3(r_3 = 1.5, \phi_3 = \pi), \mathbf{x}_4(r_4 = 1.5, \phi_4 = 3\pi/2)]$ exterior points with different intersecting angles, respectively. It is very obvious that the results of Figs. 13 and 14 are the same as those of Fig. 10. This represents that the additional exterior points with intersecting angle π provide dependent equations. At the same time, if the additional exterior points,
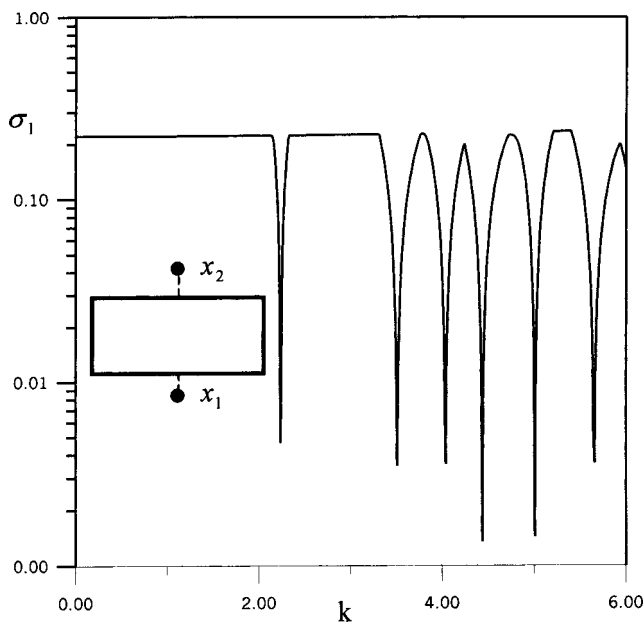

FIG. 24. Two sample points $x_1(1.0, -0.25)$ and $x_2(1.0, 1.25)$, σ_1 vs k using the real-part UT equation.
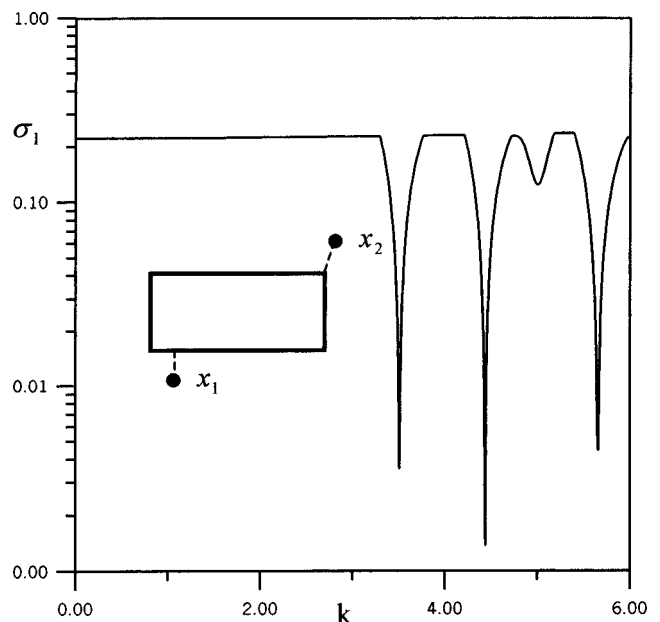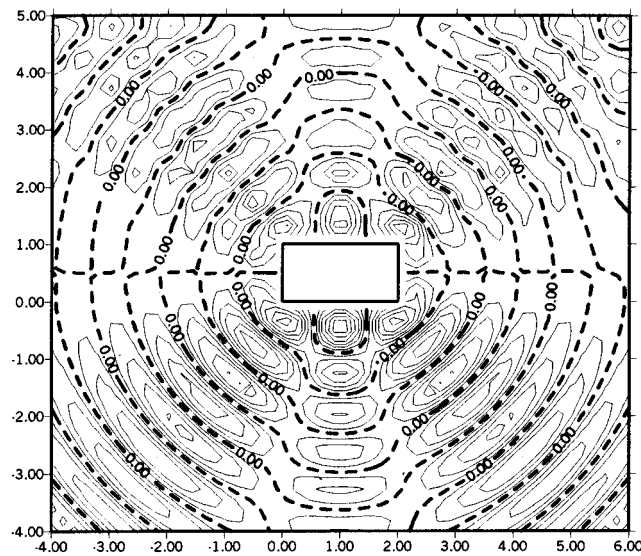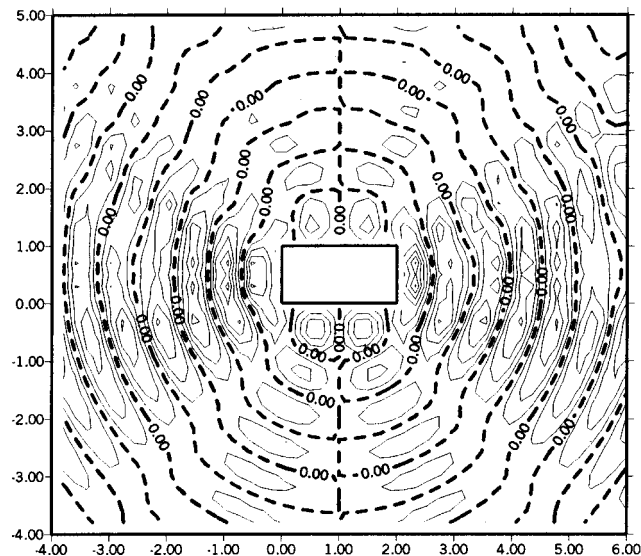

FIG. 25. Two sample points $x_1(0.3, -0.3)$ and $x_2(2.1, 1.3)$, σ_1 vs k using the real-part UT equation.

(a)

(b)

FIG. 26. (a) The spurious double root of the first radiation mode of a rectangle for the Dirichlet problem with $k_s=4.98$. (b) The spurious double root of the second radiation mode of a rectangle for the Dirichlet problem with $k_s=4.98$.

one point $\mathbf{x}_1$ with $r_1=k_{2,2}/k_{2,1}=6.794/3.384=2.007$ as described in Eq. (62) and $\phi_1=\pi/4$ and another point $\mathbf{x}_2$ with $r_2=1.4$ and $\phi_2=0$, are both chosen, then the spurious roots can be filtered out, except $Y_{2,1}$ as illustrated in Fig. 15. Figure 16 indicates that if the additional two exterior points $\mathbf{x}_1(r_1=1.5,\phi_1=0)$ and $\mathbf{x}_2(r_2=1.5,\phi_2=\pi/4)$ are carefully chosen, then all the spurious eigenvalues can be filtered out. It is interesting to find that the potential distribution is not trivial for the spurious eigenvalues; however, the potential distribution in the exterior domain for a true case is trivial, as shown in Fig. 17 $[J_{0,1}(2.405)]$ and Fig. 18 $[J_{1,1}(3.832)]$. The dotted lines in the radiation modes represent the nodal lines. The radius of these nodal lines match the data in Table II. Table II also shows that most of spurious eigenvalues with low frequencies can be filtered out efficiently by select-
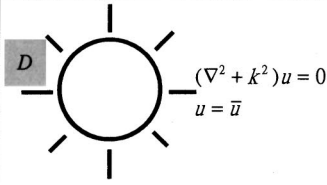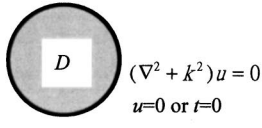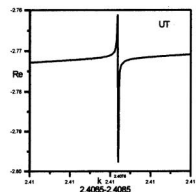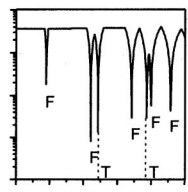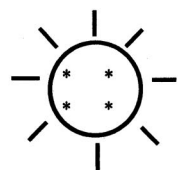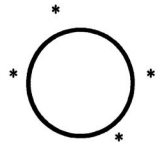
ing the points in the region of $1<r<1.24$, since the density of nodal lines in that area is low.

A rectangular cavity with length $a=2$ m and width $b=1$ m subjected to the Dirichlet boundary condition is demonstrated to see the validity for a problem with general geometry. Sixty elements in the BEM mesh were adopted. Figure 19 indicates the first and second minimum singular values, σ_1 and σ_2 vs k, where the true and spurious, single and double eigenvalues can be obtained. In the range of $0<k<6$, we have three true eigenvalues (3.51, 4.44, and 5.66) and six spurious eigenvalues [1.05, 2.23, 3.37, 3.57, 4.02, and 4.98 (double root)]. If the additional exterior point $\mathbf{x}_1(x_1=1.0,y_1=-0.25)$ is chosen, then the spurious roots can be filtered out except for the double spurious eigenvalue (4.98) and some single spurious eigenvalues (2.23, 4.02), where the selected points are on the nodal line as illustrated in Fig. 20. The spurious radiation modes of $k=2.23$ and $k=4.02$ are shown in Fig. 21 and Fig. 22. Figure 23 shows that if one additional exterior point $\mathbf{x}_1(x_1=0.25,y_1=-0.25)$ is chosen, then the spurious eigenvalues can be filtered out except for the double spurious eigenvalue $k=4.98$. Figure 24 shows that if the additional two exterior points $\mathbf{x}_1(x_1=1.0,y_1=-0.25)$ and $\mathbf{x}_2(x_2=1.0,y_2=1.25)$ are both chosen, then some spurious eigenvalues (2.23, 4.02, and 4.98) cannot be filtered out, since the additional exterior points are on the nodal line of the spurious radiation modes. If the additional two exterior points $\mathbf{x}_1(x_1=0.3,y_1=-0.3)$, $\mathbf{x}_2(x_2=0.21,y_2=1.3)$ are chosen, then all the spurious eigenvalues can be filtered out as illustrated in Fig. 25. At the same time, we know that the spurious eigenvalue of $k=4.98$ is a spurious eigenvalue with multiplicity 2, because one additional exterior point cannot work well. The two radiation modes of the spurious eigenvalue 4.98 are shown in Figs. 26(a) and (b). From these radiation mode figures, it is shown that if the additional exterior points are close to the boundary and are not located on a special position, such as on the nodal lines of $x=a/n$ or $y=b/n$ ($n\in N$), then the spurious eigenvalues can be filtered out efficiently. It is worthy to point out that the nodal lines of radiation mode for a circle can be rotated, since a circle has the property of rotation symmetry. However, the nodal lines of radiation modes for a rectangle cannot be rotated.

VII. CONCLUSIONS

The CHEEF method in conjunction with the SVD technique was applied to determine the true and spurious eigenvalues of circular and rectangle cavities subjected to the Dirichlet boundary conditions. The relationship between the CHIEF and CHEEF methods was summarized in Table III. The failure cases in selecting the exterior points for circular and rectangle cavities were studied analytically and demonstrated numerically. If the additional points are properly chosen, there are no more than two points required. The true eigenvalues obtained by the CHEEF method match very well with the exact solutions. It is very worthy to point out that the nodal line of radiation mode for a circle can be rotated due to its symmetry, whereas the nodal line of radiation

TABLE III. Comparison between the CHIEF and CHEEF methods.

Method / Description	CHIEF Combined Helmholtz Interior integral Equation Formulation	CHEEF Combined Helmholtz Exterior integral Equation Formulation
Problem statement	 $(\nabla^2 + k^2)u = 0$ $u = \bar{u}$ Radiation or scattering problem	 $(\nabla^2 + k^2)u = 0$ $u=0$ or $t=0$ eigenproblem
Method of solution	complex-valued BEM (UT or LM)	BEM (real-part or imaginary-part)
Numerical trouble	 fictitious wave number	 spurious eigenvalue
Additional constrain		
Risk	nodal lines for interior modes	nodal lines for radiation modes
Treatment	dual formulation	complex-valued formulation

mode of rectangle is on a fixed position. The multiplicity was also examined. The CHEEF method can reduce memory storage and computation time in comparison with the real-part dual BEM.

[1] H. A. Schenck, ''Improved integral formulation for acoustic radiation problems,'' J. Acoust. Soc. Am. **44**(1), 41–58 (1968).
[2] G. W. Benthien and H. A. Schenck, ''Nonexistence and nonuniqueness problems associated with integral equation method in acoustic,'' Comput. Struct. **65**, 295–305 (1997).
[3] T. W. Wu and D. W. Lobitz, ''SuperCHIEF: A modified CHIEF method,'' SANDIA Labs Report SAND-90-1266 (1991).
[4] P. Juhl, ''A numerical study of the coefficient matrix of the boundary element method near characteristic frequencies,'' J. Sound Vib. **175**(1), 39–50 (1994).
[5] S. Poulin, ''A boundary element model for diffraction of water waves on varying water depth,'' Ph.D. dissertation of Department of Hydrodynamics and Water Resources, Technical University of Denmark, ISVA Series Paper No 64, ISSN 0107-1092, Lyngby (1997).
[6] G. De Mey, ''Calculation of eigenvalues of the Helmholtz equation by an integral equation,'' Int. J. Numer. Methods Eng. **10**, 59–66 (1976).
[7] A. J. Nowak and A. C. Neves, editors, *The Multiple Reciprocity Boundary Element Method* (Comp. Mech., Southampton, 1994).
[8] G. R. G. Tai and R. P. Shaw, ''Helmholtz equation eigenvalues and eigenmodes for arbitrary domains,'' J. Acoust. Soc. Am. **56**, 796–804 (1974).
[9] G. De Mey, ''A simplified integral equation method for the calculation of the eigenvalues of Helmholtz equation,'' Int. J. Numer. Methods Eng. **11**, 1340–1342 (1977).
[10] J. R. Hutchinson, ''Determination of membrane vibrational characteristic by the boundary-integral equation method,'' in *Recent Advances in Boundary Element Method*, edited by C. A. Brebbia (Pentech, London, 1978), pp. 301–316.
[11] J. T. Chen, S. R. Kuo, and C. X. Huang, ''Analytical study and numerical experiments for true and spurious eigensolutions of a circular cavity using the real-part dual BEM,'' *IUTAM/IACM/IABEM Symposium on BEM*, Cracow, Poland, pp. 18–19 (1999).
[12] J. T. Chen, S. R. Kuo, and K. H. Chen, ''A nonsingular integral integral formulation for the Helmholtz eigenproblems of a circular domain,'' J. Chin. Inst. Chem. Eng. **22**(6), 729–739 (1999).
[13] J. T. Chen, ''Recent development of dual BEM in acoustic problems,'' Comput. Methods Appl. Mech. Eng. **188**(3–4), 1–15 (2000).
[14] J. T. Chen and F. C. Wong, ''Analytical derivations for one-dimensional eigenproblems using dual BEM and MRM,'' Eng. Anal. Boundary Elem. **20**(1), 25–33 (1997).
[15] D. Y. Liou, J. T. Chen, and K. H. Chen, ''A new method for determining the acoustic modes of a two-dimensional sound field,'' J. Chin. Inst. Civ. Hydr. Eng. **11**(2), 89–100 (1999) (in Chinese).
[16] J. T. Chen, C. X. Huang, and F. C. Wong, ''Determination of spurious eigenvalues and multiplicities of true eigenvalues in the dual multiple

reciprocity method using the singular value decomposition technique,'' J. Sound Vib. **230**(2), 203–219 (2000).

[17] W. Yieh, J. R. Chang, C. M. Chang, and J. T. Chen, ''Applications of dual BEM for determining the natural frequencies and natural modes of a rod using the singular value decomposition method,'' Adv. Eng. Softw. **30**(7), 459–468 (1999).

[18] W. Yieh, J. T. Chen, and C. M. Chang, ''Applications of dual MRM for determining the natural frequencies and natural modes of a Euler-Bernoulli beam using the singular value decomposition method,'' Eng. Anal. Boundary Elem. **23**(4), 339–360 (1999).

[19] J. T. Chen, C. X. Huang, and K. H. Chen, ''Determination of spurious eigenvalues and multiplicities of true eigenvalues using the real-part dual BEM,'' Comput. Mech. **24**(1), 41–51 (1999).

[20] J. T. Chen and H-K. Hong, ''Review of dual boundary element methods with emphasis on hypersingular integrals and divergent series,'' Appl. Mech. Rev. **52**(1), 17–33 (1999).

[21] W. Yieh, J. T. Chen, K. H. Chen, and F. C. Wong, ''A study on the multiple reciprocity method and complex-valued formulation for the Helmholtz equation,'' Adv. Eng. Softw. **29**(1), 1–6 (1997).

[22] J. R. Chang, W. Yieh, and J. T. Chen, ''Determination of natural frequencies and natural mode of a rod using the dual BEM in conjunction with the domain partition technique,'' Comput. Mech. **24**(1), 29–40 (1999).

[23] J. T. Chen and F. C. Wong, ''Dual formulation of multiple reciprocity method for the acoustic mode of a cavity with a thin partition,'' J. Sound Vib. **217**(1), 75–95 (1998).

[24] J. T. Chen, K. H. Chen, and S. W. Chyuan, ''Numerical experiments for acoustic modes of a square cavity using the dual BEM,'' Appl. Acoust. **57**(4), 293–325 (1999).

[25] J. T. Chen and H-K. Hong, *Boundary Element Method*, 2nd ed. (New World, Taipei, 1992) (in Chinese).

[26] N. Kamiya, E. Andoh, and K. Nogae, ''A new complex-valued formulation and eigenvalue analysis of the Helmholtz equation by boundary element method,'' Adv. Eng. Softw. **26**, 219–227 (1996).

[27] J. D. Jackson, *Classical Electrodynamics* (Wiley, New York, 1975).

[28] J. T. Chen, ''On fictitious frequencies using dual series representation,'' Mech. Res. Commun. **25**(5), 529–534 (1998).

[29] J. T. Chen and S. R. Kuo, ''On fictitious frequencies using circulants for radiation problems of a cylinder,'' Mech. Res. Commun. **27**(1), 49–58 (2000).

[30] J. L. Goldberg, *Matrix Theory with Applications* (McGraw-Hill, New York, 1991).